The Baryon Asymmetry from a Composite Higgs

Sebastian Bruggisser,[1] Benedict von Harling,[1] Oleksii Matsedonskyi,[1] and Géraldine Servant[1,2]

[1]*DESY, Notkestraße 85, D-22607 Hamburg, Germany*
[2]*II. Institute of Theoretical Physics, University of Hamburg, D-22761 Hamburg, Germany*

(Dated: March 26, 2018)

We study the nature of the electroweak phase transition (EWPT) in models where the Higgs emerges as a pseudo-Nambu-Goldstone boson of an approximate global symmetry of a new strongly-interacting sector confining around the TeV scale. Our analysis focusses for the first time on the case where the EWPT is accompanied by the confinement phase transition of the strong sector. We describe the confinement in terms of the dilaton, the pseudo-Nambu-Goldstone boson of spontaneously broken conformal invariance of the strong sector. The dilaton can either be a meson-like or a glueball-like state and we demonstrate a significant qualitative difference in their dynamics. We show that the EWPT can naturally be strongly first-order, due to the nearly-conformal nature of the dilaton potential. Furthermore, we examine the sizeable scale variation of the Higgs potential parameters during the EWPT. In particular, we consider in detail the case of a varying top quark Yukawa coupling, and show that the resulting CP violation is sufficient for successful electroweak baryogenesis. We demonstrate that this source of CP violation is compatible with existing flavour and CP constraints. Our scenario can be tested in complementary ways: by measuring the CP-odd top Yukawa coupling in neutron EDM experiments, by searching for dilaton production and deviations in Higgs couplings at colliders, and through gravitational waves at LISA.

INTRODUCTION

Deciphering the origin of the Higgs potential and its stabilization against quantum corrections is an essential step towards the microscopic understanding of electroweak (EW) symmetry breaking. This is one of the key questions posed by the standard model (SM) of particle physics. One of very few known options for a natural underlying dynamics is that the Higgs boson is a composite object, a bound state of a new strongly interacting sector which confines around the TeV scale [1]. The mass gap between the Higgs and the yet unobserved other composite resonances can be explained if the Higgs is a pseudo-Nambu-Goldstone boson of a global symmetry G of the strong sector which breaks down to a subgroup H due to a strong condensate χ. The Higgs mass is then protected by a shift symmetry.

Another question left unanswered by the SM is the origin of the matter-antimatter asymmetry of the universe. One fascinating framework, the EW baryogenesis mechanism [2, 3], fails in the SM due to the absence of a first-order EW phase transition (EWPT) and of sufficient CP-violation. Determining the nature of the EWPT is an indispensable step to investigate whether EW baryogenesis is the correct explanation for the baryon asymmetry of the universe.

In Composite Higgs (CH) models, since the Higgs arises only when a non-zero condensate χ forms, the confinement phase transition and the EWPT are closely linked. Nevertheless, so far, studies of the EWPT in CH models considered them separately. They either focussed on the confinement phase transition, relying on a 5D description [4–12], or assumed that the EWPT takes place after confinement of the strong sector [13–16]. The novelty of our work is to consider the interlinked dynamics between the Higgs and the condensate during the EWPT. We present a detailed analysis of the EWPT associated with the confinement phase transition, within a purely four-dimensional framework, and show that often both phase transitions happen simultaneously. In fact, this seems to be the most minimal way to obtain a strong first-order EWPT in CH models and solves the first problem of EW baryogenesis in the SM. Complementing previous studies based on 5D-dual models in which the condensate is a glueball, we also treat the meson case (motivated by lattice studies [17, 18]).

An additional attractive feature of CH models is the explanation of the hierarchy of SM Yukawa couplings as originating from the mixing between elementary and composite fermions [19, 20]. The resulting Yukawa couplings effectively depend on the confinement scale and are therefore expected to vary during the phase transition. CH models thus automatically incorporate the possibility of varying Yukawa couplings during the EWPT, which was shown to bring sufficient CP violation for EW baryogenesis [21, 22]. Furthermore, the Higgs potential in CH models is intimately tied to the top quark Yukawa coupling. Its variation then leads to a large variation of the Higgs potential, making the coupled Higgs-χ dynamics non-trivial. In this letter, we study this effect and show that sufficient CP violation is naturally induced from the varying top Yukawa, thus solving the second problem of EW baryogenesis in the SM. We therefore demonstrate that CH models can naturally give rise to EW baryogenesis, even in their simplest implementation, the so-called Minimal Composite Higgs Model.

HIGGS + DILATON PHASE TRANSITION

The Higgs potential at present times can be parametrised as a sum of trigonometric functions of h [23],

$$V^0[h] \,=\, \alpha^0 \sin^2\left(\frac{h}{f}\right) \,+\, \beta^0 \sin^4\left(\frac{h}{f}\right), \qquad (1)$$

where α^0 and β^0 are generated by sources which explicitly break G and are fixed to reproduce the mass and vacuum expectation value (*vev*) of the Higgs. The scale f, balancing the Higgs field in the trigonometric functions, is generated by the strong sector condensate. The currently preferred value is around $f = 0.8$ TeV [24] which we will use in the following. This value of f has to be linked to the condensation scale χ. The novel aspect of our work is to promote χ to a dynamical field. In well-motivated scenarios, the strong sector is nearly conformal above the TeV scale [25]. Confinement is then associated with the spontaneous breaking of conformal invariance. This gives rise to a corresponding pseudo-Nambu-Goldstone boson, the dilaton, which we identify with χ. If the dilaton is somewhat lighter than the other composite resonances, we can describe the confinement phase transition in terms of the dilaton getting a *vev*. We derive the joint potential for the Higgs and the dilaton, working in the regime where other composite resonances can be integrated out, and show under which circumstances both fields obtain a *vev* simultaneously.

The potential (1) is minimised at

$$h_0^2 \simeq -(1/2)(\alpha^0/\beta^0)f^2. \tag{2}$$

This ties the cosmological evolution of the Higgs and the dilaton to each other. In particular, the strengths of the EWPT and the confinement phase transition then become linked. Since the latter is governed by the almost conformal dilaton potential, this can naturally lead to a strong first-order EWPT, i.e. $h/T > 1$ at the transition temperature, as we will show in the following.

We describe the coupled dynamics of the Higgs and the dilaton by using a large-N expansion for the underlying strongly-coupled gauge theory [26], where N represents the number of colors. Each insertion of χ or h is accompanied by a coupling g_χ or g_*, respectively. By large-N counting, these couplings scale as $\sim 1/\sqrt{N}$ for mesons and $\sim 1/N$ for glueballs of the gauge theory. The Higgs is expected to be a meson in analogy with QCD pions while for the dilaton both meson and glueball cases are possible. Requiring a fully strongly interacting theory in the limit $N \to 1$, this gives [1]

$$g_* = g_\chi^{(\text{meson})} = 4\pi/\sqrt{N}, \qquad g_\chi^{(\text{glueball})} = 4\pi/N. \tag{3}$$

The trigonometric functions in $V^0[h]$ can be represented as power series in h/f. Using the large-N scaling together with dimensional analysis, one finds that this has to correspond to a power series in $g_* h/(g_\chi \chi_0)$, where χ_0 is the dilaton *vev* today. This fixes the relation between f and χ_0 as

$$g_* f = g_\chi \chi_0. \tag{4}$$

To account for the variation of the scale balancing h in the trigonometric functions in Eq. (1) when χ varies, the kinetic terms are fixed by dimensional analysis as

$$\mathcal{L}_{\text{kin}} = \frac{1}{2}(\chi/\chi_0)^2(\partial_\mu h)^2 + \frac{1}{2}(\partial_\mu \chi)^2. \tag{5}$$

We next turn to the Higgs-independent dilaton potential. In an exactly conformal theory, only a term χ^4 can appear which does not allow for a minimum $\chi_0 \neq 0$. We therefore break conformal invariance explicitly in the UV by a term $\epsilon\mathcal{O}$ in the Lagrangian, where $\mathcal{O}$ is an operator with scaling dimension $4+\gamma_\epsilon$. If $0 > \gamma_\epsilon \gg -1$, the coefficient ϵ slowly grows when running from the UV scale down to lower energies until it triggers conformal-symmetry breaking and confinement. This is reflected by an additional term in the dilaton potential (see e.g. [27])

$$V_\chi[\chi] = c_\chi g_\chi^2 \chi^4 - \epsilon[\chi]\chi^4 \tag{6}$$

which allows for a minimum at $\chi_0 \neq 0$. Here the function $\epsilon[\chi]$ is governed by an RG equation with β-function $\beta \simeq \gamma_\epsilon \epsilon + c_\epsilon \epsilon^2/g_\chi^2$ and c_χ and c_ϵ are order-one coefficients. We will trade γ_ϵ for the dilaton mass m_χ and fix the remaining constants as $c_\epsilon = 0.1$, and $c_\chi = 0.5$ not far from a naive order-one estimate.

To obtain a first-order phase transition, the dilaton potential needs a barrier that separates the origin from the minimum χ_0. Such a barrier (which the potential (6) does not feature) results from temperature corrections, which produce an additional minimum around $\chi = 0$. Indeed, by dimensional analysis and large-N counting, the free energy of the deconfined phase is given by [4–6]

$$\Delta V_T[\chi = 0] \sim -cN^2T^4 \,. \tag{7}$$

We choose $c = \pi^2/8$, a value corresponding to $\mathcal{N} = 4$ $SU(N)$ super-Yang-Mills that is representative of a realistic conformal sector. We reproduce this free energy at $\chi = 0$ by including the standard one-loop thermal corrections from $45N^2/4$ strongly coupled bosonic degrees of freedom with mass $m = g_\chi \chi$ [5] (Using fermions would only marginally change the shape of the potential.) At high temperatures, this dip traps the dilaton at $\chi = 0$. As the temperature drops, it eventually tunnels to the global minimum at $\chi \simeq \chi_0$ corresponding to a confined phase.

Altogether, the potential of our model reads

$$V_{\text{tot}}[h,\chi] = (\chi/\chi_0)^4 V_h^0[h] + V_\chi[\chi] + \Delta V_T^{\text{1-loop}}[h,\chi]\,, \tag{8}$$

where the prefactor χ^4 of the Higgs potential follows from dimensional analysis since the dilaton *vev* is the only source of mass in the theory. Furthermore, $\Delta V_T^{\text{1-loop}}$ includes the one-loop thermal corrections from SM particles, the Higgs and dilaton as well as the states reproducing the free energy (7).

We have calculated the tunnelling trajectory and action for $O(3)$-symmetric bubbles in the two-dimensional field space (h,χ). The phase transition happens at a temperature T_n for which the bubble action is $S_3/T_n \approx 140$. In Fig. 1, we show examples of tunneling trajectories. An important quantity for EW baryogenesis is the strength of the phase transition $h[T_n]/T_n$, where $h[T_n]$ is at the minimum of the Higgs potential at T_n. To ensure that sphalerons do not wash out the generated baryon asymmetry, $h[T_n]/T_n \gtrsim 1$ is required.

In the left panel of Fig. 2, we show how the strength of the EWPT depends on N and the dilaton mass for both a meson-like and a glueball-like dilaton (the used parameters will be discussed in the next section). Generally, the phase transition quickly becomes supercooled with growing N and decreasing dilaton mass, as found in previous studies of the confinement phase transition focussing on the glueball, e.g. [12]. This effect is stronger for the glueball due to the different N-scaling of its couplings. Overall, our results show that there is ample parameter space for which the EWPT is sufficiently strong.

We will find in the next section that the parameters α^0 and β^0 in Eq. (1) can significantly depend on χ. This effect is already taken into account in Figs. 1 and 2 but turns out to have little impact on the size of the tunnelling action and therefore on the strength of the phase transition in most of the parameter space. However, it strongly affects the tunnelling direction, which controls the size of the CP-violating source that we now discuss.

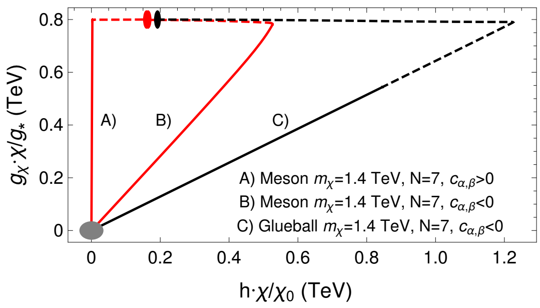

Figure 1: *Examples of transition trajectories for different dilaton properties. Solid lines show the tunnelling path to the release point, while dotted lines indicate the subsequent rolling trajectory towards the minimum of the potential at T_n, indicated by a bullet in each case.*

CP VIOLATION FROM VARYING TOP MIXING

A sufficient amount of CP asymmetry can be generated during the EWPT from the phase variation of the top quark Yukawa coupling [21]. This CP-violating source was considered previously in non-minimal CH models, where an additional singlet scalar field gives another contribution to the top Yukawa [15], and in a 5D model [28]. However, here we do not rely on these extra ingredients. In CH models, the fermion masses originate from linear interactions between the elementary fermions q_i and composite sector operators $\mathcal{O}_i$:

$$y_i \bar{q}_i \mathcal{O}_i . \tag{9}$$

The dimensionless coefficients y_i are assumed to be of order one in the UV, where the mixings are generated. They run subject to an RG equation with β-function $\gamma_i y_i + c_i y_i^3/g_*^2$, where c_i are order-one coefficients and the scaling dimension of the operator $\mathcal{O}_i$ is given by $5/2 + \gamma_i$. The anomalous dimensions γ_i can remain sizeable over a large energy range due to an approximate conformal symmetry (see *e.g.* [25]). The RG evolution stops at the confinement scale $\sim \chi$, where the operators map to composite states. This makes the mixings y_i dependent on χ. Integrating out the composite states, one obtains the effective SM Yukawa couplings

$$\lambda_q[\chi] \sim y_{qL}[\chi]\, y_{qR}[\chi]/g_* , \tag{10}$$

where L and R denote the mixings of the left- and right-handed elementary fermions, respectively. In this framework, the SM fermion mass hierarchy is then explained by order-one differences in the scaling dimensions of the operators in Eq. (9). This also offers a natural way to make the top Yukawa λ_t vary during the phase transition, as the condensation scale then changes.

For the CP-violating source to be non-vanishing, however, λ_t needs to vary not only in absolute value but also in phase [21]. To achieve this, we will assume that the right-handed top couples to two different operators in the UV:

$$y_{tR}^{(1)} \bar{t}_R \mathcal{O}_1 + y_{tR}^{(2)} \bar{t}_R \mathcal{O}_2 \;\; \Rightarrow \;\; \lambda_t \sim y_{tL}(y_{tR}^{(1)} + y_{tR}^{(2)})/g_* . \tag{11}$$

Provided that $y_{tR}^{(1,2)}$ are complex and $\mathcal{O}_{1,2}$ have different scaling dimensions (which we assume to be the case), the phase of λ_t changes with χ. This provides a source of CP violation, but also has another crucial effect on the phase transition which we now explain.

The largest contribution to the Higgs potential in CH models typically arises from the top quark mixings. We assume that only one of the mixings $y_{tR}^{(1,2)}$, which we denote as y, varies sizeably with the dilaton *vev*. Its one-loop contribution to the coefficients α^0 and β^0 in Eq. (1) reads

$$\alpha[\chi] = c_\alpha \, \frac{3y^2[\chi]g_*^2}{(4\pi)^2} f^4, \quad \beta[\chi] = c_\beta \, \frac{3y^2[\chi]g_*^2}{(4\pi)^2} f^4 \left(\frac{y[\chi]}{g_*}\right)^{p_\beta}, \tag{12}$$

where c_α and c_β are free parameters of our effective field theory, expected to be of order one. Furthermore, $p_\beta = 0, 2$ depending on the structure of the elementary-composite mixings [23, 32] (we choose $p_\beta = 0$ for definiteness). Note that the contributions from the top mixings are somewhat larger than the coefficients α^0 and β^0 in Eq. (1) which reproduce the observed Higgs mass and *vev*. This points to the well-known tuning required to obtain the observed Higgs mass and *vev* in CH models: Additional contributions to α^0 and β^0 must partially cancel those in Eq. (12). However, we can expect this cancellation to happen only when the mixings have their values today and thus, as the mixings depend on χ, only for $\chi = \chi_0$. In order to take this into account, we make the replacement [23]

$$\alpha^0 \to \alpha^0 + (\alpha[\chi] - \alpha[\chi_0]), \quad \beta^0 \to \beta^0 + (\beta[\chi] - \beta[\chi_0]) \tag{13}$$

in Eq. (1). Furthermore, since the mixings explicitly break the conformal invariance of the CH sector, we include an additional contribution $\propto y^2 \chi^4$ in the dilaton potential (which only plays a subdominant role though).

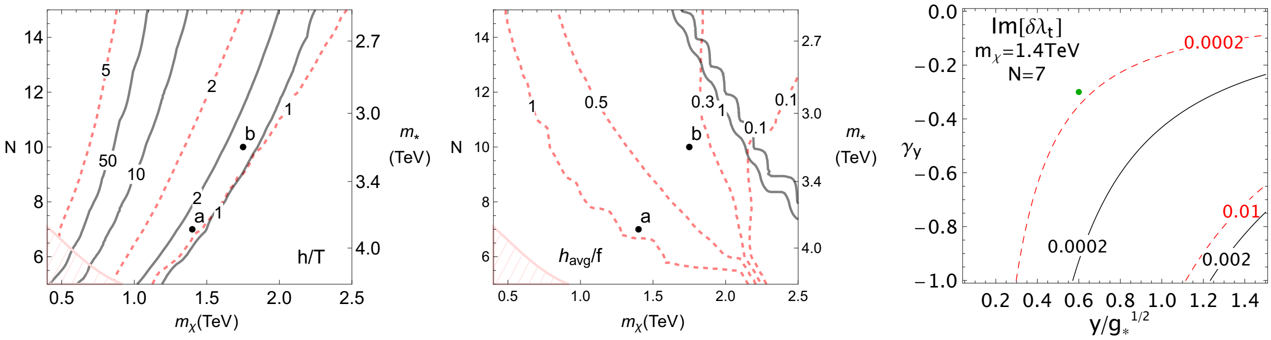

Figure 2: *Black solid (red dashed) contours are for a glueball (meson) dilaton. In the red dashed region, there is no phenomenologically viable EW minimum for the case of the meson dilaton. We also show the values of the cutoff $m_* = g_* f$. The chosen mass range satisfies current experimental constraints [29]. Left: Phase-transition strength $h[T_n]/T_n$. The baryon asymmetry for a meson (glueball) like dilaton is $|\eta_B| \times 10^{10} \sim 7$ (3) (a), 2 (6) (b). Center: Average Higgs* vev *during the phase transition relative to the condensate scale today, $h_{\rm avg}/f$. Right: Imaginary part of the top Yukawa as a function of the present value of $y/g_*^{1/2}$ and its anomalous dimension γ_y for $|\beta_y| = \gamma_y y$, a complex phase* $\arg \beta_y = 0.1$ *and $y_{tL} = \sqrt{g_*}$. The current and near future experimental sensitivities correspond respectively to approximately* 2×10^{-2} *[30] and* 2×10^{-4} *[31]. The green bullet indicates the values used for the left and centre plots.*

To have the minimum of the Higgs potential at $h_0 \ll f$ at present times requires that $|\alpha^0/\beta^0| \ll 1$. From Eq. (12), on the other hand, we see that generically $|\alpha[\chi]/\beta[\chi]| \gtrsim 1$. This is a manifestation of the required tuning mentioned before. For χ somewhat away from χ_0, the contributions in Eq. (12) typically dominate over α^0 and β^0 in Eq. (13) and the Higgs potential instead has a global minimum at $h = 0$ (for $c_{\alpha,\beta} > 0$) or $h = f\pi/2$ (for $c_{\alpha,\beta} < 0$). This minimum leads to a valley in the Higgs-dilaton potential which can attract the tunneling trajectory during a first-order phase transition. How closely the tunneling trajectory follows this valley is controlled by its relative depth (in particular determined by m_χ and N) and the value of χ for which it becomes deeper than the valley along $h = h_0$ that results from the tuned Higgs potential (1) (influenced by $|c_{\alpha,\beta}|, \gamma_y, y[0], y[\chi_0]$). Different tunnelling trajectories are shown in Fig. 1. The form of the trajectory has major implications for EW baryogenesis. In particular, trajectories which closely follow $h = 0$ need to be avoided since the top mass and thus the CP-violating source vanish along such trajectories. This can also happen for trajectories which closely follow $h = f\pi/2$, however, since the fermion masses are $\propto \sin[h/f]^{1+m} \cos[h/f]^n$ [33] with m, n being model-dependent, and therefore vanish at $h = f\pi/2$ if $n \neq 0$.

The top mixings are already quite large at $\chi = \chi_0$ to ensure a large top Yukawa. Provided that the anomalous dimension γ_y for the mixing y is negative, it grows for decreasing χ until it reaches a fixed point whose size is controlled by the constant c_y in the β-function. To obtain a sufficient amount of y variation and CP violation, we choose $\gamma_y = -0.3$ and fix c_y so that $y[0] = 0.4 g_*$ in the unbroken phase, while $y[\chi_0] = 0.6\sqrt{\lambda_t g_*}$ in the broken phase. We also set $c_\alpha = c_\beta = -0.3$ in which case the detuned valley is along $h = f\pi/2$. We have calculated the action of $O(3)$-symmetric bubbles for tunneling along straight lines with constant Higgs *vev* h which well approximates the exact tunneling paths (cf. Fig. 1). In the central panel of Fig. 2, we plot the Higgs *vev* $h_{\rm avg}$ which minimizes the action at the transition temperature. We see that, depending on m_χ and N, different trajectories are possible for the meson case. In contrast, the glueball-like dilaton either follows $h = 0$ or $h = f\pi/2$ with a sharp transition in between. Notice that in the case of $h = f\pi/2$ the CP-violating source is non-vanishing only in models with $n = 0$.

Thus, as follows from the first two panels in Fig. 2, the EWPT is strong and our CP-violating source is active for a wide range of m_χ and N. We have computed the resulting baryon asymmetry using the formalism presented in Ref. [21]. The results are indicated for a few benchmark points, assuming a bubble wall velocity of 0.01 (the baryon asymmetry increases by a factor 3-4 if we increase the bubble wall velocity to 0.1) and with the varying mixing in Eq. (11) having a complex phase $\arg y_{tR}^{(1)} = \arg y[\chi] = 0.1$ and the remaining mixings being fixed as $y_{tR}^{(2)} \simeq 0.4\sqrt{\lambda_t g_*}$ and $y_{tL} = \sqrt{\lambda_t g_*}$. Note that even in the region where $h[T_n]/T_n \gtrsim$ a few, we can expect subsonic velocities as a sizeable friction comes from the large number of degrees of freedom becoming massive when they go through the bubble wall. Our baryon asymmetry values (which should only be taken as indicative given order one uncertainties) are typically 2 to 8 times bigger than the observed value $\eta_B \sim 8.5 \times 10^{-11}$. In contrast with phase transitions studied so far, our Higgs *vev* grows very large during the EWPT before decreasing, and since η_B scales as the integral of $(h/T)^2$ over the bubble wall, this leads to a large baryon asymmetry. Furthermore, we find that the bubble wall width L_w is small, also contributing to a large baryon asymmetry. However, we actually enter a regime where the derivative expansion used in the EW baryogenesis formalism ($L_w T \gg 1$) [21] starts to break down.

EXPERIMENTAL SIGNATURES

Our predictions can be divided into two types - those related to the phase-transition strength (only weakly sensitive to the y running), and those related to the transition path and CP violation (strongly sensitive to the y running). For the former, our testable prediction is the correlation between the dilaton mass and the strong-sector coupling, from the requirement of a strong enough EWPT, see Fig. 2. As for the latter, the running mixing y can have a measurable effect on both the Higgs and the dilaton phenomenology, as well as on observables which are indirectly sensitive to the couplings of h and χ. Many of these effects arise from the term responsible for the top mass, which in the meson case with $n = 0$ reads

$$\lambda_t[\chi]\,\chi\,\sin\frac{h}{f}\,\bar{t}_L t_R \supset \bar{t}_L t_R\, h\left(\lambda_t^0\frac{\chi}{f} + \beta_{\lambda_t}\frac{\chi - f}{f}\right), \quad (14)$$

where λ_t^0 is the SM top Yukawa coupling, and for one varying mixing we have $\beta_{\lambda_t} \sim \beta_y$ (see Eq. (10)). This expression needs to be rewritten in terms of the mass eigenstates, rotated with respect to h and χ with an angle which also depends on β_y, since y enters into the scalar potential (8). Importantly, once λ_t^0 is chosen to be real, its β-function is complex, as required by the varying Yukawa phase. The highest sensitivity to the resulting complex couplings comes from measurements of the neutron electric dipole moment [34]. These restrict modifications of the CP-odd top Yukawa coupling to be $\lesssim 2 \times 10^{-2}$ at 95% CL [30], with a prospect of gaining about two orders of magnitude in sensitivity in the near future [31]. In the right panel of Fig. 2, we show how the CP-odd tth coupling depends on $y[\chi]$. Constraints will be more stringent for the meson dilaton than for the glueball. The forthcoming experiments are expected to probe a significant fraction of our parameter space.

In the longer term, future colliders can probe deviations in the Higgs couplings arising from the mixing with the dilaton [35] and a stochastic background of gravitational waves peaked in the milli-Hertz range can be searched for at LISA [5, 35].

In summary, our results strongly support the viability of EW baryogenesis and motivate further studies in concrete calculable realizations of CH models. In a forthcoming paper [35], we extend this analysis to other possible sources of CP violation, such as from the interplay of the top and charm mixings, and discuss the resulting relations between CP violation, flavour symmetries and the structure of the elementary-composite mixings.

[1] G. Panico and A. Wulzer, Lect. Notes Phys. **913**, pp.1 (2016), 1506.01961.

[2] D. E. Morrissey and M. J. Ramsey-Musolf, New J. Phys. **14**, 125003 (2012), 1206.2942.

[3] T. Konstandin, Phys. Usp. **56**, 747 (2013), [Usp. Fiz. Nauk183,785(2013)], 1302.6713.

[4] P. Creminelli, A. Nicolis, and R. Rattazzi, JHEP **03**, 051 (2002), hep-th/0107141.

[5] L. Randall and G. Servant, JHEP **05**, 054 (2007), hep-ph/0607158.

[6] G. Nardini, M. Quiros, and A. Wulzer, JHEP **09**, 077 (2007), 0706.3388.

[7] B. Hassanain, J. March-Russell, and M. Schvellinger, JHEP **10**, 089 (2007), 0708.2060.

[8] T. Konstandin, G. Nardini, and M. Quiros, Phys. Rev. **D82**, 083513 (2010), 1007.1468.

[9] T. Konstandin and G. Servant, JCAP **1112**, 009 (2011), 1104.4791.

[10] D. Bunk, J. Hubisz, and B. Jain (2017), 1705.00001.

[11] B. M. Dillon, B. K. El-Menoufi, S. J. Huber, and J. P. Manuel (2017), 1708.02953.

[12] B. von Harling and G. Servant, JHEP **01**, 159 (2018), 1711.11554.

[13] C. Delaunay, C. Grojean, and J. D. Wells, JHEP **04**, 029 (2008), 0711.2511.

[14] B. Grinstein and M. Trott, Phys. Rev. **D78**, 075022 (2008), 0806.1971.

[15] J. R. Espinosa, B. Gripaios, T. Konstandin, and F. Riva, JCAP **1201**, 012 (2012), 1110.2876.

[16] M. Chala, G. Nardini, and I. Sobolev, Phys. Rev. **D94**, 055006 (2016), 1605.08663.

[17] Y. Aoki et al. (LatKMI), Phys. Rev. **D89**, 111502 (2014), 1403.5000.

[18] T. Appelquist et al., Phys. Rev. **D93**, 114514 (2016), 1601.04027.

[19] D. B. Kaplan, Nucl. Phys. **B365**, 259 (1991).

[20] R. Contino, T. Kramer, M. Son, and R. Sundrum, JHEP **05**, 074 (2007), hep-ph/0612180.

[21] S. Bruggisser, T. Konstandin, and G. Servant, JCAP **1711**, 034 (2017), 1706.08534.

[22] G. Servant, Phil. Trans. Roy. Soc. Lond. **376**, 20170124 (2018).

[23] G. Panico, M. Redi, A. Tesi, and A. Wulzer, JHEP **03**, 051 (2013), 1210.7114.

[24] C. Grojean, O. Matsedonskyi, and G. Panico, JHEP **10**, 160 (2013), 1306.4655.

[25] R. Contino, in *Physics of the large and the small, TASI 09, proceedings of the Theoretical Advanced Study Institute in Elementary Particle Physics, Boulder, Colorado, USA, 1-26 June 2009* (2011), pp. 235–306, 1005.4269, URL `https://inspirehep.net/record/856065/files/arXiv:1005.4269.pdf`.

[26] E. Witten, Nucl. Phys. **B160**, 57 (1979).

[27] E. Megias and O. Pujolas, JHEP **08**, 081 (2014), 1401.4998.

[28] B. von Harling and G. Servant, JHEP **05**, 077 (2017), 1612.02447.

[29] K. Blum, M. Cliche, C. Csaki, and S. J. Lee, JHEP **03**, 099 (2015), 1410.1873.

[30] V. Cirigliano, W. Dekens, J. de Vries, and E. Mereghetti, Phys. Rev. **D94**, 034031 (2016), 1605.04311.

[31] K. Kumar, Z.-T. Lu, and M. J. Ramsey-Musolf, in *Fundamental Physics at the Intensity Frontier* (2013), pp. 159–214, 1312.5416, URL `https://inspirehep.net/record/1272872/files/arXiv:1312.5416.pdf`.

[32] O. Matsedonskyi, G. Panico, and A. Wulzer, JHEP **01**, 164 (2013), 1204.6333.

[33] A. Pomarol and F. Riva, JHEP **08**, 135 (2012), 1205.6434.

[34] J. M. Pendlebury et al., Phys. Rev. **D92**, 092003 (2015), 1509.04411.

[35] S. Bruggisser, B. von Harling, O. Matsedonskyi, and G. Servant (2018).